

## Fusion between heavy ions at sub-barrier energies

Q. Haider and F. Bary Malik

*Department of Physics and Astronomy, Southern Illinois University at Carbondale,  
Carbondale, Illinois 62901*

(Received 1 April 1982)

The  $S$  factors for the capture process of the systems  $^{16}\text{O}+^{16}\text{O}$ ,  $^{16}\text{O}+^{14}\text{N}$ ,  $^{16}\text{O}+^{12}\text{C}$ ,  $^{14}\text{N}+^{14}\text{N}$ ,  $^{14}\text{N}+^{12}\text{C}$ ,  $^{11}\text{B}+^{12}\text{C}$ , and  $^{10}\text{B}+^{12}\text{C}$  are calculated at sub-Coulomb barrier energies in a model using an inverted parabola which joins smoothly onto the Coulomb potential between two heavy ions. The model does not have any discontinuous potential surface and has proper asymptotic forms for the wave functions and has been successful in understanding fusion cross sections at higher energies. The calculated energy dependence of the  $S$  factor follows in general the experimental trend and in many instances, the observed magnitudes can be reproduced remarkably well.

[ NUCLEAR REACTIONS Heavy-ion fusion; sub-barrier region;  $S$  factor calculations for  $^{16}\text{O}+^{16}\text{O}$ ,  $^{16}\text{O}+^{14}\text{N}$ ,  $^{16}\text{O}+^{12}\text{C}$ ,  $^{14}\text{N}+^{14}\text{N}$ ,  $^{14}\text{N}+^{12}\text{C}$ ,  $^{11}\text{B}+^{12}\text{C}$ , and  $^{10}\text{B}+^{12}\text{C}$ . ]

In recent papers,<sup>1,2</sup> we have provided a formalism for heavy-ion fusion as penetration through a parabolic barrier joining smoothly to the Coulomb interaction. The formalism is valid for all energies and avoids the discontinuous potential surface present in the calculations of Avishai<sup>3</sup> and Dethier and Stancu.<sup>4</sup> It would be natural to extend that formalism to study the fusion between two light heavy ions at sub-barrier energies. The understanding of fusion phenomenon at sub-barrier energies is of particular interest in astrophysics because of recently proposed theories suggesting that such processes might provide important insight into nucleosynthesis of elements. In addition, the small Coulomb barrier associated with light ions has made it possible to measure with great precision the fusion cross sections at sub-Coulomb barrier energies. Hence, an understanding of these data is likely to provide further information about the reaction mechanism, particularly for tracing the shape of the ion-ion potential in the low-energy region.

Several theoretical investigations<sup>3-6</sup> have already attempted to calculate the  $S$  factor defined as

$$S = \sigma_f E \exp(2\pi\eta), \quad (1)$$

where  $\sigma_f$  is the fusion cross section and  $\eta$  is the Sommerfeld parameter related to the wave number  $k$ , reduced mass  $\mu$ , and charges  $Z_1e$  and  $Z_2e$  of the two nuclei by

$$\eta = \mu Z_1 Z_2 e^2 / (\hbar^2 k).$$

$E$  is the center of mass energy of the colliding ions.  $\sigma_f$  is related to the penetrability function  $T_l(E)$  by the equation

$$\sigma_f = (\pi/k^2) \sum_{l=0}^{\infty} (2l+1) T_l(E). \quad (2)$$

Except for the potential of Michaud,<sup>6</sup> which is of the complex Woods-Saxon type with a Gaussian repulsive core, most of the works describe fusion as penetration through a one-dimensional real inverted parabolic barrier. However, at the sub-Coulomb barrier energies, the Coulomb interaction is likely to play a big role in determining the penetrability function because the energy is well below the barrier height. As noted earlier, Avishai<sup>3</sup> and Dethier and Stancu<sup>4</sup> attempted to incorporate penetration through a Coulomb barrier by modifying the Hill-Wheeler expression<sup>7</sup> for transmission through a parabolic barrier. Their treatment, apart from having validity in a limited energy range, results in having ultimately a discontinuous potential.

Our treatment,<sup>1</sup> apart from incorporating Coulomb interaction properly and using a continuous potential surface where the Coulomb potential joins smoothly to an inverted parabola, uses proper boundary condition and asymptotic forms of the wave functions. The theory has been able to reproduce the gross part of the observed fusion cross sections for a number of systems at incident energies above the barrier height. In this work, we extend our earlier calculations to the sub-barrier energy re-

gion and examine the extent to which the theory can reproduce the magnitude and trend, such as the energy dependence of the observed cross section. Our purpose here is, therefore, not to provide a perfect fit to the data but to explore the extent of the success and failure of the model of Ref. 1.

To facilitate the discussion, we briefly outline the barrier used in Ref. 1. It is given by

$$V_l(r) = \begin{cases} V_l - \frac{1}{2}\mu\omega^2(r - R_0)^2, & r < R_n \\ Z_1 Z_2 e^2 / r + \hbar^2 l(l+1) / (2\mu r^2), & r > R_n \end{cases} \quad (3a)$$

$$(3b)$$

where  $R_n = r_n(A_1^{1/3} + A_2^{1/3})$  is the distance between the two ions when they are about to touch each other and  $A_1$  and  $A_2$  are their respective mass numbers.  $\hbar\omega$  is the oscillator constant determining the curvature of the parabola.  $V_l$  is determined from the matching condition at  $r = R_n$  and is given by

$$V_l = V_0 + \hbar^2 l(l+1) / (2\mu R_n^2) \quad (4)$$

with

$$V_0 = \frac{1}{2}\mu\omega^2(R_n - R_0)^2 + Z_1 Z_2 e^2 / R_n. \quad (5)$$

Thus  $R_0$  locates the  $s$ -wave barrier height  $V_0$ . The model has three free parameters, namely,  $\hbar\omega$ ,  $V_0$ , and  $R_n$  (or  $r_n$ ). The probability of transmission,  $T_l(E)$ , is calculated by matching the logarithmic derivative of the wave functions in the two regions at  $r = R_n$ . The wave function for  $r > R_n$  is expressed in terms of the regular and irregular Coulomb functions, while for  $r < R_n$ , the wave function is taken to be a linear combination of parabolic cylinder functions. Details of the calculations are given in Ref. 1.

In the following, we apply the above model to calculate the  $S$  factor (in MeV b) for the reactions  $^{16}\text{O} + ^{16}\text{O}$ ,  $^{16}\text{O} + ^{14}\text{N}$ ,  $^{16}\text{O} + ^{12}\text{C}$ ,  $^{14}\text{N} + ^{14}\text{N}$ ,  $^{14}\text{N} + ^{12}\text{C}$ ,  $^{11}\text{B} + ^{12}\text{C}$ , and  $^{10}\text{B} + ^{12}\text{C}$ . We use the reaction  $^{16}\text{O} + ^{16}\text{O}$  as a test case for studying (a) the effect of approximating the barrier by a pure parabola, and (b) the effect of discontinuity on the potential surface which is present in the models of Avishai<sup>3</sup> and Dethier and Stancu.<sup>4</sup> These are shown in Fig. 1. The dashed curve in the figure represents calculations using the parabolic potential model of Glas and Mosel.<sup>8</sup> The potential parameters are taken from the work of Kolata *et al.*<sup>9</sup> From the figure,

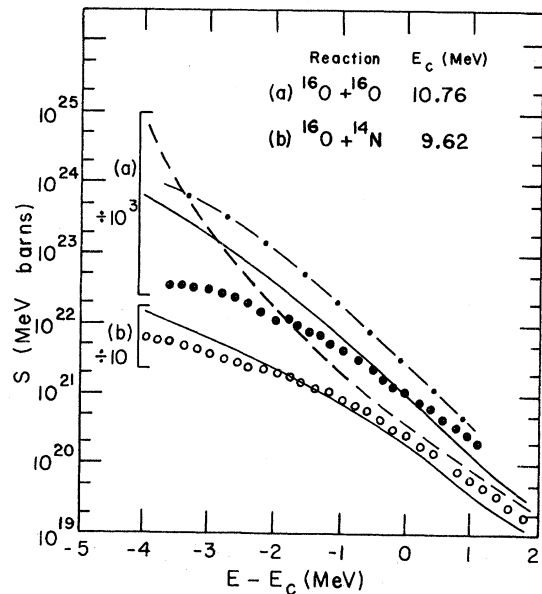


FIG. 1. A comparison between the predicted and experimentally measured values of the  $S$  factor for the reactions  $^{16}\text{O} + ^{16}\text{O}$  and  $^{16}\text{O} + ^{14}\text{N}$ . The data are taken from Ref. 10 and are denoted by solid circles for  $^{16}\text{O} + ^{16}\text{O}$  and open circles for  $^{16}\text{O} + ^{14}\text{N}$ . The solid lines, the upper one for  $^{16}\text{O} + ^{16}\text{O}$  and the lower one for  $^{16}\text{O} + ^{14}\text{N}$ , are the results of the present work. The dashed curve represents results obtained for  $^{16}\text{O} + ^{16}\text{O}$  by using a purely parabolic potential (Glas-Mosel model) and the dashed-dotted curve shows the effect of inclusion of Coulomb interaction but with a discontinuity in the potential (Avishai model) for the same reaction.

it is clear that the omission of the Coulomb interaction in the sub-barrier region results not only in an overestimation of the data in the low-energy region, but also gives the wrong shape of the data. As noted later, the reason for this is that a parabolic barrier does not represent the true shape of the potential in the low-energy region. The dashed-dotted curve represents calculations using the model and parameters of Avishai<sup>3</sup> but modifying it to incorporate the proper boundary condition and asymptotic forms of the wave functions, as outlined in Ref. 1. From the figure, it is apparent that a discontinuous potential would consistently overpredict the data with the disagreement becoming larger in the extremely low-energy region. Such overpredictions have also been noted by Dethier and Stancu.<sup>4</sup> However, the reproduction of the correct shape of the data in Avishai's model is a consequence of the presence of the Coulomb interaction.

Similar behavior for the Glas-Mosel and Avishai models is also noted for the reaction  $^{16}\text{O} + ^{14}\text{N}$ , though they are not shown in the figure. The solid curves represent calculations, for both  $^{16}\text{O} + ^{16}\text{O}$  and  $^{16}\text{O} + ^{14}\text{N}$  reactions, using the model of Ref. 1 as described by Eqs. (3a) and (3b). This model also reproduces the correct shape, primarily because of the inclusion of the Coulomb potential. The values of the parameters are the same as those used in Ref. 1 for energies greater than the barrier height. We note that it would be possible to obtain a better fit to the data by slightly adjusting the values of the parameters. However, we chose not to do so because that would have obscured the simple fact that it is possible to approximately reproduce the shape and magnitude of the data, both below and above the barrier, by the same set of parameters. The values of the parameters used in the calculations are listed in Table I.

In Fig. 2, we present our calculations together with the experimental data of Cujec and Barnes<sup>5</sup> for the reaction  $^{16}\text{O} + ^{12}\text{C}$ . It is found that the calculated results are unable to predict the structures present in the data in the energy region below 6.0 MeV. But above 6.0 MeV, the quality of agreement is comparable to the optical model fit obtained by using the potential of Michaud.<sup>6</sup> Figure 3 shows the comparison between our predicted results and the experimental results of Stokstad *et al.*<sup>10</sup> for the reactions  $^{14}\text{N} + ^{14}\text{N}$ ,  $^{14}\text{N} + ^{12}\text{C}$ ,  $^{11}\text{B} + ^{12}\text{C}$ , and  $^{10}\text{B} + ^{12}\text{C}$ . Except for  $^{10,11}\text{B} + ^{12}\text{C}$ , the calculated results in all other cases slightly overpredict the measured  $S$  factor at the lowest energies.

The tendency to overpredict the  $S$  factors, particularly for the reaction  $^{16}\text{O} + ^{16}\text{O}$ , at energies well

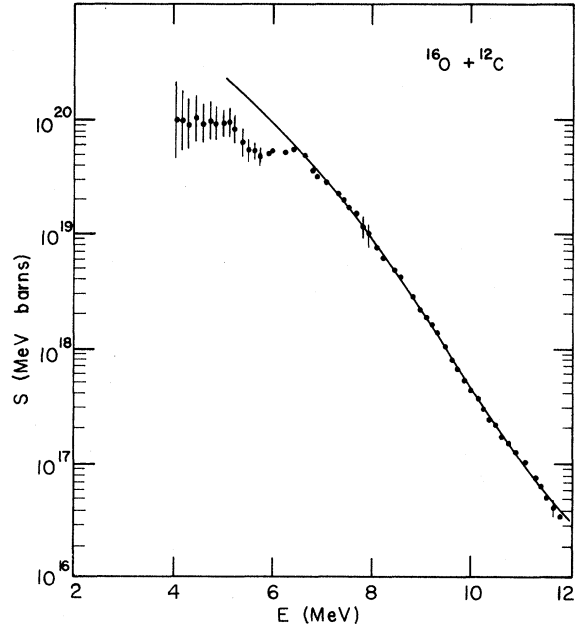


FIG. 2. A comparison between the calculated (solid line) values of the  $S$  factor with the data (solid circles) of Cujec and Barnes (Ref. 5) for the reaction  $^{16}\text{O} + ^{12}\text{C}$ .

below the Coulomb barrier is clearly a manifestation that the barrier used here is too thin near the few MeV region. Since the exterior part of the potential at those energies is primarily of the Coulomb type, and has been incorporated properly, the problem lies in the use of a simple parabolic potential to describe the inner part of the barrier. This is obvious if the parabolic potentials used here are compared with the real part of the molecular potentials used to describe the elastic scattering data of  $^{16}\text{O} + ^{16}\text{O}$  and  $^{12}\text{C} + ^{12}\text{C}$  systems.<sup>11,12</sup> Parabolas used here are a good approximation to the shape near the top of the barrier but fall off faster than the actual potential in the interior region. Thus, transmission probabilities calculated using parabolic potentials determined from high energy data are likely to be larger than those for the actual potential at very low energies. At the lowest energies, one is either to use slightly different parameters for the parabolic potential or use the real part of the actual potential itself with proper boundary conditions described in Ref. 1.

As mentioned before, it is not difficult to fit any individual set of data by changing the potential parameters used to analyze the data at higher ener-

TABLE I. Values of the parameters  $\hbar\omega$ ,  $V_0$ , and  $r_n$  used in the calculations. In the Glas-Mosel model, there are two additional parameters. They are critical distance  $R_c = 4.69$  fm and critical potential  $V_c = -10.0$  MeV.

Reaction	$\hbar\omega$ (MeV)	$V_0$ (MeV)	$r_n$ (fm)	$R_0$ (fm)
$^{16}\text{O} + ^{16}\text{O}$	7.50	13.00	1.587	7.48
Glas-Mosel	5.00	11.00		7.56
Avishai	4.62	10.92		8.00
$^{16}\text{O} + ^{14}\text{N}$	7.50	12.75	1.318	6.25
$^{16}\text{O} + ^{12}\text{C}$	7.50	12.00	1.352	5.96
$^{14}\text{N} + ^{14}\text{N}$	7.50	11.55	1.359	6.15
$^{14}\text{N} + ^{12}\text{C}$	7.50	11.50	1.329	5.60
$^{11}\text{B} + ^{12}\text{C}$	7.50	9.25	1.329	5.27
$^{10}\text{B} + ^{12}\text{C}$	7.50	9.50	1.294	5.02

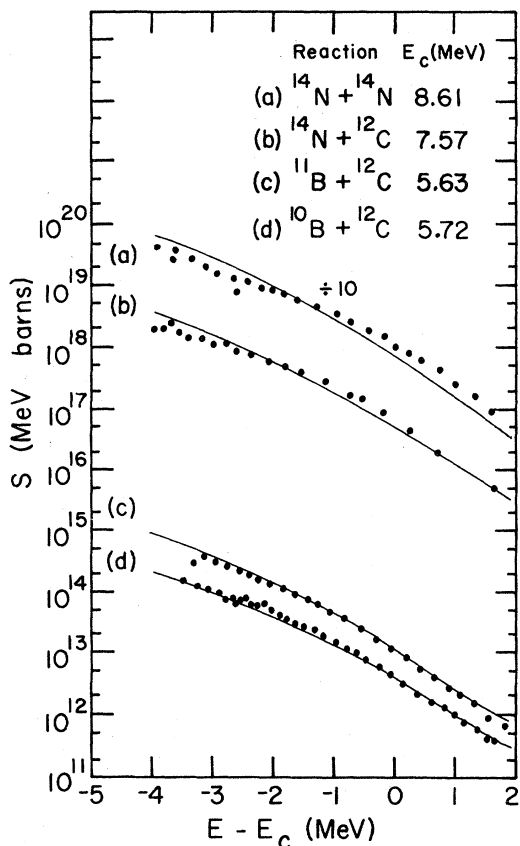


FIG. 3. A comparison between the calculated (solid lines) and experimental values (Ref. 10) of the  $S$  factor for the reactions (a)  $^{14}\text{N} + ^{14}\text{N}$ , (b)  $^{14}\text{N} + ^{12}\text{C}$ , (c)  $^{11}\text{B} + ^{12}\text{C}$ , and (d)  $^{10}\text{B} + ^{12}\text{C}$ . The experimental values are denoted by solid circles.

gies. By keeping  $\hbar\omega$  fixed at 7.5 MeV, the model, for a given set of nuclei, has used only two free parameters,  $V_0$  and  $R_n$ , which are kept fixed at all energies. Nevertheless, the model not only predicts the energy dependence of the  $S$  factor correctly, but also follows the data in many cases remarkably well. The model, as already noted,<sup>13</sup> is not suitable to understand bumps or structures in the cross sections but is geared to explaining the smooth gross features. An extension of the model to incorporate resonant behavior would be necessary to explain the observed structures, and is being formulated.<sup>13</sup>

In conclusion, we note that (1) fusion cross section at low energies is mostly dominated by the tail of the potential which is properly represented by Coulomb interaction; (2) removal of discontinuity in the potential results in a reduction in magnitude of the calculated cross section thereby improving agreement with the data; and (3) calculations in the low-energy region are sensitive to the shape of the potential, as can be seen from the slight overestimation of the data in the extremely low-energy region. Finally, we would like to point out that the low-energy fusion data, particularly in the vicinity of the Coulomb barrier, may be used as a useful guide to probe the detail shape and interior of the ion-ion potential.

One of us (Q.H.) would like to thank the Office of Research Development and Administration of Southern Illinois University at Carbondale for their financial support.

<sup>1</sup>Q. Haider and F. B. Malik, Phys. Rev. C **26**, 162 (1982).  
<sup>2</sup>F. B. Malik and Q. Haider, Bull. Am. Phys. Soc. **26**, 636 (1981).  
<sup>3</sup>Y. Avishai, Z. Phys. A **286**, 285 (1978).  
<sup>4</sup>J. -L. Dethier and Fl. Stancu, Phys. Rev. C **23**, 1503 (1981).  
<sup>5</sup>B. Cujec and C. A. Barnes, Nucl. Phys. **A266**, 461 (1976).  
<sup>6</sup>G. C. Michaud, Astrophys. J. **175**, 751 (1972); Phys. Rev. C **8**, 525 (1973).  
<sup>7</sup>D. L. Hill and J. A. Wheeler, Phys. Rev. **89**, 1102 (1953).  
<sup>8</sup>D. E. Glas and U. Mosel, Nucl. Phys. **A237**, 429 (1975).  
<sup>9</sup>J. J. Kolata, R. M. Freeman, F. Haas, B. Heusch, and

A. Gallmann, Phys. Rev. C **19**, 2237 (1979).  
<sup>10</sup>R. G. Stokstad, Z. E. Switkowski, R. A. Dayras, and R. M. Wieland, Phys. Rev. Lett. **37**, 888 (1976).  
<sup>11</sup>Q. Haider and F. B. Malik, *Proceedings of the International Conference on Resonant Behavior of Heavy-Ion Systems, Aegean Sea, 1980*, edited by G. Vourvopoulos (Greek Atomic Energy Commission, Athens, 1981), p. 501; F. B. Malik and I. Reichstein, *Proceedings of the Workshop on High Resolution Heavy-Ion Physics at 20–100 MeV/A, Saclay, 1978*, p. 61.  
<sup>12</sup>Q. Haider and F. B. Malik, J. Phys. G **7**, 1661 (1981).  
<sup>13</sup>F. B. Malik and Q. Haider, Bull. Am. Phys. Soc. **27**, 551 (1982).